Development 124, 721-729 (1997)
Printed in Great Britain © The Company of Biologists Limited 1997
DEV2129

Altered cellular proliferation and mesoderm patterning in Polycomb-M33-deficient mice

Nathalie Coré[1], Sophie Bel[1], Stephen J. Gaunt[2], Michel Aurrand-Lions[1], Jonathan Pearce[2], Amanda Fisher[3] and Malek Djabali[1,*]

[1]Centre d'immunologie INSERM-CNRS de Marseille Luminy, Case 906, 13288 Marseille Cedex 9, France
[2]The Babraham Institute, Babraham Hall, Babraham, Cambridge, CB2 4AT, UK
[3]MRC Clinical Sciences Centre, Royal Postgraduate Medical School Hammersmith Hospital, Du Cane Road, London W12 0NN, UK

*Author for correspondence

SUMMARY

In *Drosophila*, the trithorax-group and the Polycomb-group genes are necessary to maintain the expression of the homeobox genes in the appropriate segments. Loss-of-function mutations in those groups of genes lead to misexpression of the homeotic genes resulting in segmental homeotic transformations. Recently, mouse homologues of the Polycomb-group genes were identified including *M33*, the murine counterpart of *Polycomb*. In this report, *M33* was targeted in mice by homologous recombination in embryonic stem (ES) cells to assess its function during development. Homozygous *M33 (–/–)* mice show greatly retarded growth, homeotic transformations of the axial skeleton, sternal and limb malformations and a failure to expand in vitro of several cell types including lymphocytes and fibroblasts. In addition, *M33* null mutant mice show an aggravation of the skeletal malformations when treated to RA at embryonic day 7.5, leading to the hypothesis that, during development, the *M33* gene might play a role in defining access to retinoic acid response elements localised in the regulatory regions of several *Hox* genes.

Key words: *M33*, Polycomb-group genes, *Hox* genes, anteroposterior specification, cellular proliferation

INTRODUCTION

In *Drosophila*, the complex pattern of homeotic gene (HOM-C) expression is established early in development by the transiently expressed maternal and segmentation genes (Ingham, 1988). Late in development, two groups of genes are necessary to maintain the expression pattern of the homeotic genes. The trithorax group (trx-G) (reviewed by Kenisson, 1993) is required in maintaining the activity of the HOM-C genes in the appropriate segments, whereas the Polycomb group genes (Pc-G) are involved in the repression of the homeotic genes in the pertinent segments (reviewed by Paro, 1990; Bienz and Müller, 1995; Pirrotta, 1995). Loss-of-function mutations in members of the Pc-G genes result, as the expression of the segmentation genes decreases, in ectopic expression of the HOM-C genes late in embryogenesis whereas the early expression is not affected (Duncan and Lewis, 1982; Jürgens, 1985). This leads to shifts in the anterior limits of expression of the homeotic genes and, as a result, to posterior homeotic transformations. The binding of Pc to inactive *HOM/lacZ* transgenes (Zink et al., 1991) and the identification of a domain involved in chromatin binding shared with the heterochromatin protein HP1 (chromodomain) in the PC protein (Paro and Hogness, 1991), together with the co-localization of several Pc-G proteins on polytene chromosomes (DeCamillis et al., 1992) to homeotic loci, has led to the proposition that Pc-G proteins are associated in large multimeric complexes which stably repress target genes by compacting the chromatin in a condensed structure inaccessible to specific transactivators (Paro, 1990). This compacted chromatin is thought to function as the basis for cellular memory during several cellular divisions maintaining HOM-C genes in an inactive state in specific cells (Paro, 1990).

Recently, mouse homologues related to the Pc-G genes were identified (Tagawa et al., 1990; Brunk et al., 1991; van Lohuizen et al., 1991), including the *M33* gene which is considered as the structural (Pearce et al., 1992) and functional counterpart of the *Pc* gene since the *M33* gene is able to partially rescue the *Pc* mutant phenotype (Müller et al., 1995).

To gain further insight into the functions of the M33 protein, we have generated a mutant mouse lacking the M33 protein. *M33* mutant mice show homeotic transformations of the axial skeleton reminiscent of the *bmi-1* and *mel-18* mutant mice, as well as a failure to expand by several cell types, including lymphocytes and fibroblasts. Moreover, *M33* mutants show an enhanced skeletal phenotype when treated with RA indicating that the M33 protein might play a role in defining access to retinoic acid response elements (RARE) defined in the regulatory regions of several *Hox* genes.

MATERIALS AND METHODS

Construction of the targeting vector

A *Xba*I-*Eco*RI fragment containing the pGK-neo gene flanked with two loxP sites, was subcloned in the *Eco*RV site of pBluescript (pBS) SK vector (Stratagene). Two DNA fragments from the *M33* locus (Pearce et al., 1992) were isolated from a λ phage screened from a mouse 129/Ola genomic library: the 4.2 kb *Eco*RI-*Sal*I fragment contains part of the 5′ non-coding region of the *M33* gene, just upstream the start of transcription; the 3.5 kb *Xho*I-*Xba*I fragment, from the 3′ region, contains intron 4 and the last exon (exon 5). After filling the ends of restriction sites, the two *M33* homologous fragments were cloned respectively in the *Sal*I and *Xba*I sites of the modified pBS-neo vector, on each side of the loxP-neo-loxP cassette. This targeting vector pBS-neo-M33 was designed to allow the excision of exon 1 to exon 4 after homologous recombination in ES cells.

ES cells, targeting, DNA and RNA analysis

2×10^7 E14 (129/Ola) strain ES cells were electroporated with 20 μg pBS-neo-M33 targeting construct DNA. 24 hours later, cells were positively selected with 300 μg/ml G418. Isolated G418-resistant colonies were picked after 7 days of selection. Homologous recombinants were tested by hybridization of *Hin*dIII-digested genomic DNA using a *Sma*I-*Eco*RI fragment (probe E) as an external probe and part of the exon 5 as an internal probe. A unique integration event was checked with a neomycin probe. For RT-PCR analysis, RNA was extracted from kidney and PCR amplification was performed using primers 1 and 2 on exon 5 (Fig. 1A).

Skeletal analysis

Whole-mount skeletons of newborns were stained as described (Lufkin et al., 1992). 14.5 d.p.c. embryos were stained with the same protocol except for the time in 1% KOH, which was reduced to 0.5 hour. Genotyping was done by Southern blotting using genomic DNA extracted from the tail (new born) or from foetal liver.

In situ RNA analysis

In situ hybridization on sagittal sections of 12.5 d.p.c. embryos was performed according to the procedure described (Gaunt et al., 1988). Hox probes (Hoxa-3, Hoxd-3, Hoxa-5, Hoxc-5, Hoxa-6, Hoxc6, Hoxc-8) were previously described (Gaunt et al., 1988).

Flow cytometric analysis

Single cell suspensions from thymus were incubated at 1×10^7 cells/ml in 100 μl of staining solution (PBS complemented with 0.2% foetal calf serum (FCS) and 0.2% mouse serum) for 30 minutes on ice with phycoerythrin (PE)-conjugated anti CD8a (53-6.7) and biotin-conjugated anti-CD4 (H129.19) monoclonal antibodies. After two washes in PBS/0.2% FCS solution, the cells were incubated with 50 μl of Streptavidin-Cy-Chrome reagent in staining solution for 30 minutes on ice. The stained cells were washed three times and then fixed in 150 μl of 1% paraformaldehyde in PBS. Analysis were performed on a Becton Dickinson FACScan. The monoclonal antibodies and the Streptavidin-Cy-chrome reagent were purchased from PharMingen.

To establish organ cultures, thymuses were isolated from 14 d.p.c. embryo's, cultured in the presence of 1.35 mM dGuo to deplete endogenous lymphocytes and reconstituted in hanging drops with 1×10^5 foetal liver cell suspensions from 12.5 d.p.c. *M33*+/+, *M33*+/– and *M33*–/– mice. These samples contained equivalent numbers of T cell precursors as determined by serial titration. Unbound cells were removed by washing the lobes transferred to floating filters and cultured for up to 3 weeks before being individually harvested and analysed.

Proliferation assays

The fibroblasts derived from 12.5 d.p.c. *M33*+/+ and *M33*–/– were cultured for no longer than four passages in Dulbecco's modified medium (DMEM from Sigma) supplemented with 10% of heat-inactivated foetal calf serum. Cells were arrested by incubating them for 2 days in DMEM without serum. They were stimulated by adding 20% of serum and then plated in a 24-well plate for counting over a 2 week period. For activation assay, splenocytes were seeded at a concentration of 10^6 cells/ml in a 96-well plate. Cells were incubated in 200 μl of DME, 10% FCS, 10 mM Hepes pH 7.4 solution supplemented with 10 μg/ml of LypoPolySaccharide (LPS, Sigma). After 48 hours of incubation at 37°C, [^{3}H]thymidine was added at a final concentration of 5 μCi/ml. Incorporation of [^{3}H]thymidine was measured after 24 hours by scintillation counting.

Retinoic acid treatment

Retinoic acid (RA) experiments were done with animals from times matings. Animals were mated for 2 hours, and fertilisation was assumed to have occurred after 1 hour. RA in vegetal oil was administered by a single oral gavage, applying 40 mg/kilogram of body weight all trans RA (sigma).

RESULTS

Generation of *M33* mice

The murine *Polycomb* gene (*M33*) was disrupted by homologous recombination deleting the four first exons of the gene and inserting a neomycin-resistance (neo) gene in reverse orientation to the *M33* transcription (Fig. 1A). Loss of the chromodomain encoded by the first three exons abolishes *Pc* activity in *Drosophila* resulting in homeotic transformation (Messmer et al., 1992). Two independent, homologous recombinant E14 ES cell clones were obtained. Recombinant ES clones were injected into BALB/c blastocysts and reimplanted into pseudopregnant females to produce chimaeric offspring. Germ-line transmission was obtained after a backcross between chimaeric males and BALB/c females. The heterozygous and homozygous offsprings were genotyped as described above. Genomic Southern analysis (Fig. 1B) as well as reverse transcriptase polymerase chain reaction (RT-PCR), confirmed the loss of the *M33* 5′ region and the absence of the *M33* transcript in the homozygous *M33*–/– mice. (Fig. 1C).

M33 mutation leads to postnatal lethality

M33–/– mutant mice develop to term and appear normal. They represent 24% of the offspring indicating that mutant mice do not die during embryogenesis. After a few hours following

Table 1. Skeletal and growth abnormalities of 3-week-old M33−/− mice

	+/+	+/–	–/–
(a) Weight (g)	12.1±1.5 (*n*=6)		3.2±0.5 (*n*=4)
(b) Skeletal abnormalities	(*n*=9)	(*n*=9)	(*n*=13)
Exoccipital/C1 fusion	0	0	13
C2→C1	0	0	13
6 vertebrosternal ribs	0	0	13
L6→S1 one side	0	0	2
Scapula one side	0	0	7
both sides	0	0	6
(c) Number of cells ($\times10^6$)			
Thymus	210	220	1.4
Spleen	20	20	1.5

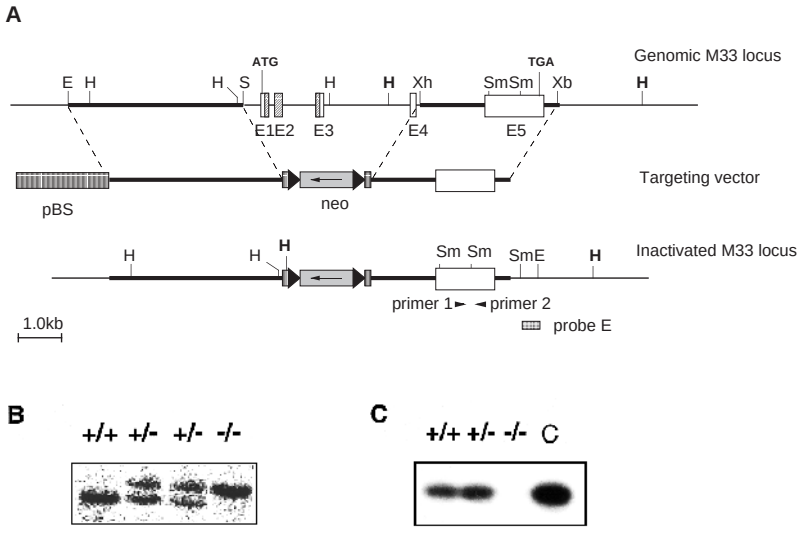

Fig. 1. Homologous recombination at the *M33* locus in embryonic stem (ES) cells. (A) Top panel, structure of the targeting vector and partial restriction map of the *M33* locus before and after targeted integration. The targeting vector contains the neomycin-resistance gene flanked by *M33* sequences. After the recombination event, the neomycin-resistance gene replaces a *Sal*I-*Xho*I fragment containing the four first exons of the *M33* gene. E, *Eco*RI; H, *Hin*dIII; Sm, *Sma*I; Xb, *Xba*I; Xh, *Xho*I. (B) Southern blot analysis of a representative litter showing alleles from a wild-type (+/+), an heterozygous (+/–) and an homozygous (–/–) animal. Hybridization of genomic DNA with an external probe (probe E) reveals a 6.5 kb *Hin*dIII fragment for the *M33* wild-type allele and a 7.2 kb *Hin*dIII fragment corresponding to the inactivated allele. (C) RT-PCR analysis of new-born wild type, heterozygotes and homozygotes from kidney RNA. Lane C is a positive PCR control on *M33* cDNA showing the amplified band with the indicated primers. No amplification can be detected from homozygous-derived RNA.

birth, half of all the *M33–/–* offspring die; after a few days, the surviving *M33–/–* mice can be easily recognised by their growth retardation (Table 1) and a high rate of lethality. Most of the *M33* mutant mice (90%) die within 4 weeks and the life span does not exceed 6 weeks.

Skeletal abnormalities

Whole-mount skeletal analysis of *M33–/–* mice reveals several malformations along the anteroposterior axis demonstrating the importance of the *M33* gene in pattern formation (Table 1). Alizarin red and alcian blue staining (Lufkin et al., 1992) of new-born and 4-week-old animals indicates that all the *M33–/–* mice analysed show a malformation of the exoccipital (ex) bone and that the atlas (C1) is missing (Fig. 2B), resulting in six cervical vertebrae instead of seven in control mice (Fig. 2A). Partial transformation of C2 to C1, as

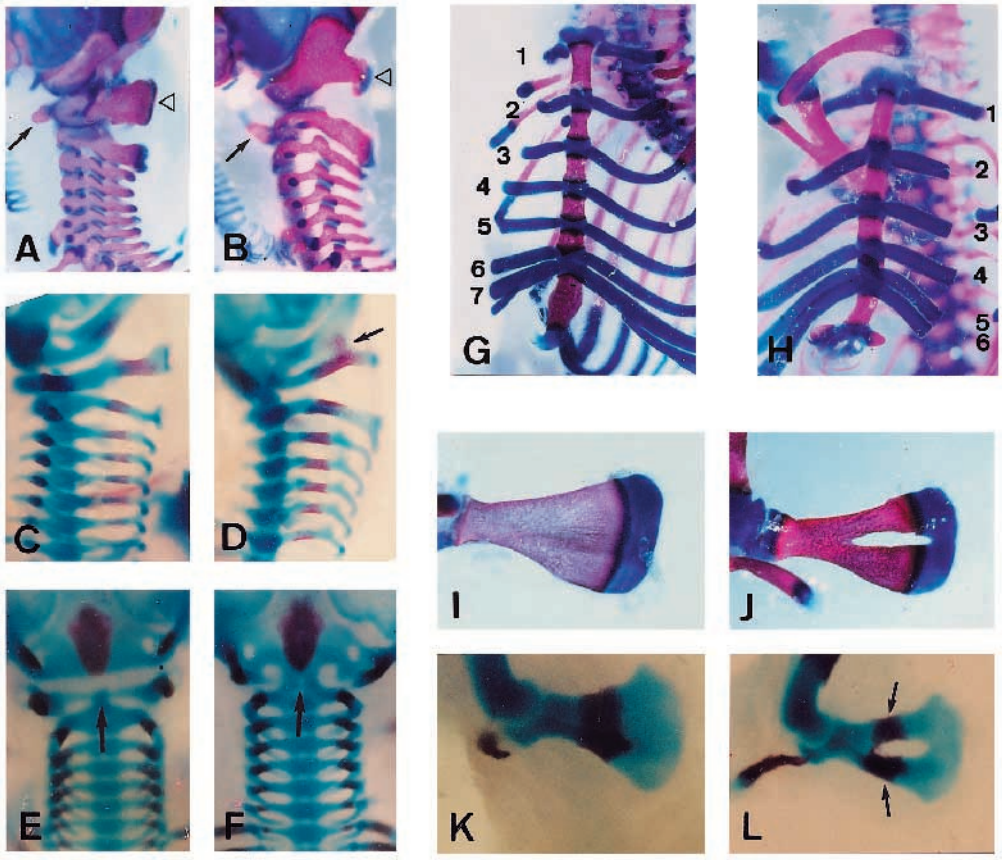

Fig. 2. Skeletal defects in *M33–/–* mice. Lateral views of cleared skeletons of new born mice (A,B,G-J) and 14.5 d.p.c. embryos (C-F,K,L). (A) Wild type, the first cervical vertebra (atlas) is indicated by an open triangle; the arrow shows the anterior arch of the atlas. (B) *M33–/–*, the atlas is shown to be fused to the exoccipital bone; the anterior arch of the atlas is shifted on to the axis (C2) as indicated by the arrow. (C) *M33+/+* embryo showing the ossification centres of the exoccipital, basioccipital and the atlas. (D) *M33–/–* embryo: the arrow indicates the fusion of the basioccipital and C1 ossification centres. (E,F) Ventral view of the same embryo as in C and D. (E) The basioccipital , the exoccipital and the atlas ossification centres can be clearly seen (arrow). (F) *M33–/–* the fusion of the atlas to the basioccipital bone is indicated (arrow). (G) Ventral view of the thoracic region of wild-type skeleton. Seven vertebrosternal ribs and six sternebrae are shown. (H) *M33–/–* thoracic region, six vertebrosternal ribs and five sternebrae are shown. The most caudal rib attached to the sternum is the sixth in the mutant and the seventh in the wild type. (I) Morphology of a wild-type scapula. (J) *M33–/–* scapula presenting a hole. (K) Wild-type scapula showing one ossification center. (L) *M33–/–* scapula; the cartilage primordium presents an abnormal hole. The arrows indicate the neoformed ossification centres.

indicated by the presence of an anterior arch of the atlas on the second cervical vertebrae was also observed in mutant mice. *M33–/–* animals show a posteriorisation of the thoracic vertebra T7 into T8, resulting in the presence of six vertebrosternal ribs instead of seven in *M33*+/+ mice (Fig. 2G,H). In addition, 15% of the mutant mice show a transformation of the lumbar vertebra L6 into a first sacral vertebra (S1) (Table 1). These transformations result in a C6/T13/L5 configuration in mutant mice in comparison to the C7/T13/L6 in wild-type mice.

Examination of 14.5 d.p.c. mutant foetuses indicates that the exoccipital/atlas malformation arises as a result of fusion between the ossification centres of these two bones (Fig. 2D). This shift induces a major remodeling of the craniocervical joint, as the first cervical vertebra is now fused to the basioccipital bone (Fig. 2F). In addition, the homozygous mice display an incomplete scapula formation resulting in a split ossification centre (Fig. 2J). At 14.5 d.p.c., the cartilage primordium of the scapula is already affected and two ossification centres are present on each side of the scapula (Fig. 2L). The altered morphogenesis of the scapula in *M33–/–* mice is actually reminiscent of normal pelvic bone development where the ossification centres of the ischial and pubic bones fuse anteriorly, giving the pelvic bone a triangular shape with a central hole (obturator foramen).

Hox genes expression in *M33* mutant mice

Regulation of *Hox* gene expression boundaries is critical for specification of vertebral identities in mouse (McGinnis and Krumlauf, 1992). The Polycomb group genes, *mel-18* (Akasaka et al., 1996) and *bmi-1* (van der Lugt et al., 1994; Alkema et al., 1995), have been shown to regulate the anterior limits of expression of some of the *Hox* genes and to induce homeotic transformations in loss-of-function or gain-of-function experiments. Posterior or anterior transformations of vertebrae have been described in the case of *Hox* gene gain of functions or loss of functions in mice (McGinnis and Krumlauf, 1992). These data prompted us to examine the expression patterns of some representative *Hox* genes in the *M33–/–* mice. By RNA in situ hybridisation, *Hoxa-3* transcript was detected over the basioccipital bone anlage in mutant mice (Fig. 3B) but not in wild-type mice (Fig. 3A). This anterior shift in the *Hoxa-3* boundary is widened by the fusion of the basioccipital and the first prevertebra (Pv1), which was already manifest at 12.5 d.p.c. of development (Fig. 3B). However, we found no significant differences in the anterior limits of expression of several other *Hox* genes in the mutant mice. As shown in Fig. 3C,D the boundaries for *Hoxc-8* and *Hoxc-6* are normal (Gaunt et al., 1988) if we assume that the first discernible prevertebra is Pv2 (Pv1 having become fused with the occipital). Similarly, the anterior boundaries for *Hoxd-4 Hoxa-5, Hoxc-5* and *Hoxa-6* (pv2, 3, 6 and 8, respectively) are not affected in the mutant mice (data not shown). Moreover the boundaries for all these *Hox* genes appear at apparently normal positions in the central nervous system (Fig. 4) (Gaunt et al., 1988). Fig. 4 also shows that there are no ectopic areas of Hox gene expression located anterior to the boundaries. This finding is in contrast to that made for *Drosophila Polycomb*$^{-/-}$ embryos (Wedeen et al., 1986) and suggests that, unlike Pc in *Drosophila*, M33 protein in mice is not critical for the maintenance of all *Hox* expression domains.

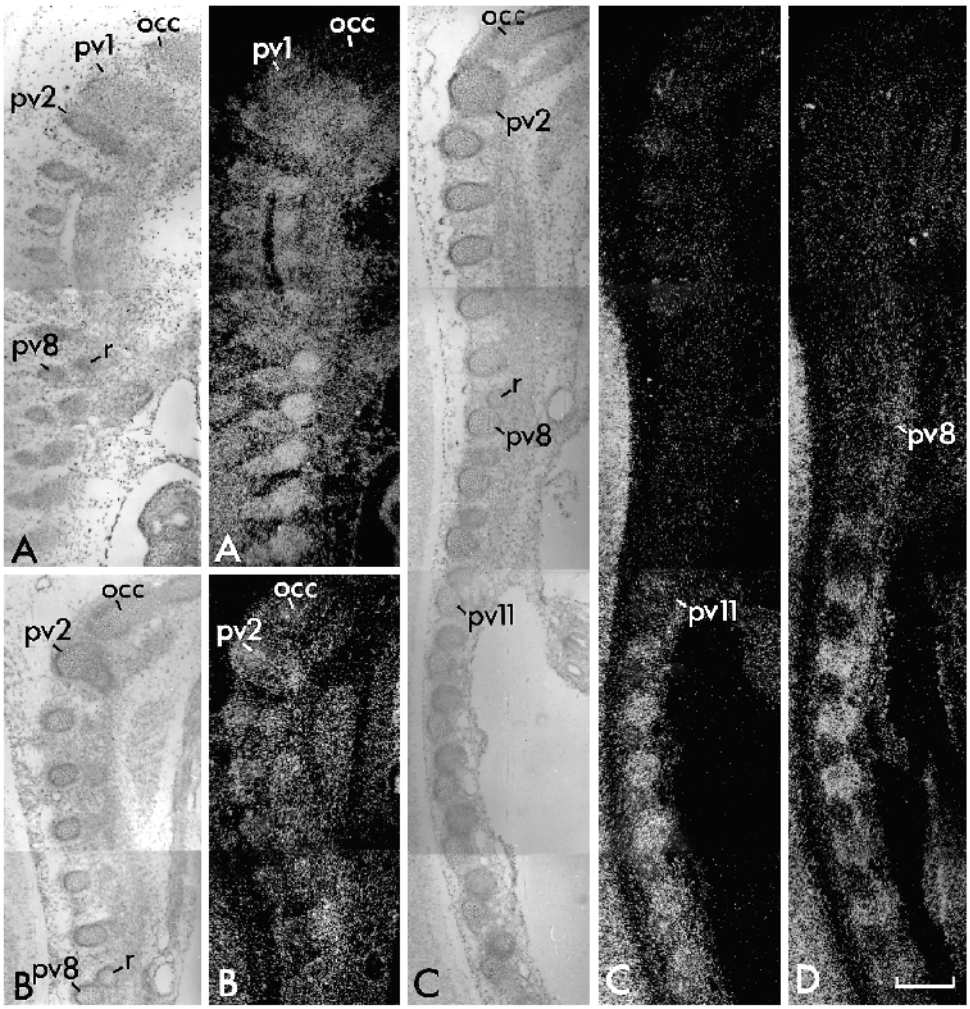

Fig. 3. Hox gene expression within the prevertebral column of normal (A) and *M33–/–* (B-D) 12.5 d.p.c embryos. (A,B) *Hoxa-3*; (C) *Hoxc-8*; (D) *Hoxc-6*. Note that the anterior boundary of the *Hoxa-3* expression domain is shifted anteriorly by one segment whereas the *Hoxc-8* and *Hoxc-6* are not. Fields are shown by bright-field (left) and dark-field (right) illumination. Sections (parasagittal) B, C and D were cut from the same embryo. occ, basioccipital; pv, prevertebra; r, first rib. Scale bar, 0.2 mm.

RA treatment analysis

It has been suggested that the normal boundaries of *Hox* gene expression might normally be regulated by retinoic acid and that ectopic expression of the *Hox* genes induced by RA administration leads to morphological transformations (Kessel and Gruss, 1991; Conlon and Rossant, 1994). The recent identification of retinoic response elements (RARE) in the regulatory region of *Hox* genes (Langston and Gudas, 1992) has provided direct evidence for an involvement of RA in the regulation of *Hox* genes during development. In order to test whether the M33 protein plays a role in the accessibility of the RARE, we administered RA to 7.5 d.p.c. pregnant *M33+/–* females bred with *M33+/–* males. Pregnant females were killed at 17.5 d.p.c. and the morphological changes were scored in *M33+/+*, *M33+/–* and *M33–/–* embryos and compared to the untreated *M33–/–* embryos. As shown in Fig. 5, the skeletal alterations seen in the *M33–/–* mice are largely amplified in the *M33–/–* RA-treated embryos. Althought the effects of RA in the cervical region in the *M33* mutants are difficult to interpret (since RA induces by itself in wild-type mice strong malformations in the cervical region; Kessel and Gruss, 1991), the additional effects of RA can be more easily seen in the thoracic region of the *M33* mutant mice. The *M33–/–* RA-treated mice present three sternebrae ossification centres instead of five in the *M33–/–* untreated animals (Fig. 5A). The xiphoid process of the treated mutant is split in two parts. Moreover the treated mutant mice display only five sternebrae; the first two being fused before joining the manubrium sterni. In addition, the scapula defect detected in the *M33–/–* mutant (Fig. 5D) is also severely enhanced by the RA treatment (Fig. 5C). These changes were not induced in the *M33+/+* mice and were induced only weakly in *M33+/–* mice (Fig. 5B). Heterozygotes did not show these changes in the absence of retinoic acid (Table 1).

Lymphocyte abnormalities

Examination of 3- and 4-week-old *M33–/–* animals showed pronounced involution of the thymus and spleen with a drastic reduction in the total number of nucleated cells in these organs (>100 fold and >10 fold, respectively; Table 1). To assess which cell types were affected, flow cytometric analysis (FACS) was performed on thymocytes using standard lymphoid markers (Fig. 6A). The presence of single positive cells (SP) (CD4+ or CD8+) expressing normal level of T-cell receptor (data not shown) showed that T cell development can progress in the absence of *M33*. However the relative proportions and number of each T cell subset were disturbed in *M33–/–* mice as compared with controls; immature CD4–/CD8– thymocytes account for 25% of cells in *M33–/–* thymuses suggesting that these precursors are either retarded in their normal differentiation pathway as a direct effect of the absence of *M33* or alternatively that the failure to thrive and general poor health of the *M33–/–* animals accounts for the diminishing population CD4+/CD8+ DP cell population. To establish the cause of reduced thymocyte numbers and CD4+8+ subsets in *M33–/–* mice, thymic organ cultures were used to estimate the frequency and the differentiation potential of T cell precursors in vitro. Foetal liver cells from 12.5 d.p.c. embryos were used to recolonise alymphoid (dGuo-treated) thymic lobes (Cohen and Duke, 1984), and the development of T cells was monitored by FACS. Serial titration experiments showed that the relative abundance of pro-T cells in foetal liver of *M33–/–*, heterozygotes and wild-type mice, was equivalent at days 12-14 d.p.c., (data not shown). A marked reduction in T cell expansion was observed in cultures derived from *M33–/–* mice as illustrated in Fig. 6C. Over a two weeks culture period, the number of T cells recovered per lobe increased from 1×10^4 to 2.6×10^5 in wild-type and heterozygote samples, compared with an increase from 1×10^4 to 5.1×10^4 in samples established from *M33–/–* mice. This reduction was accompanied by a slight retardation in T cell maturation (Fig. 6B), although representatives of all stages of T cell development were observed. These data show that pro-T cells in *M33–/–* mice appear at normal

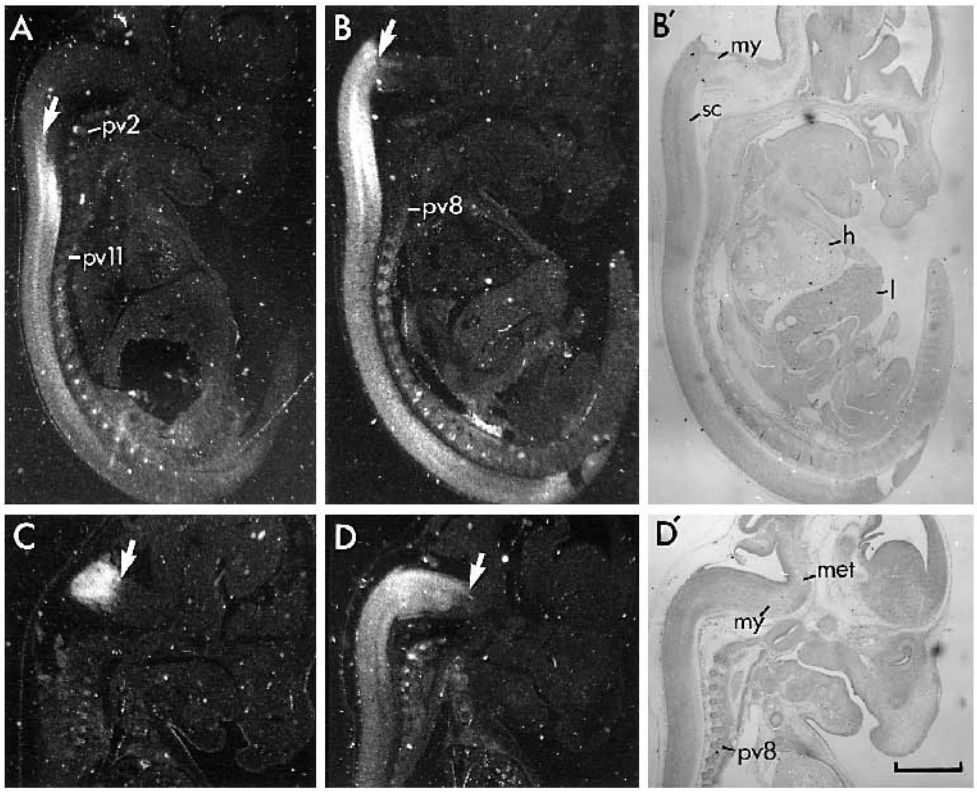

Fig. 4. Hox gene expression within the central nervous system of *M33–/–* 12.5 d.p.c embryos. (A-D) Dark-field and (B′,D′) corresponding bright-field illumination. In situ hybridization on sagittal sections were realized with *Hoxc-8* (A), *Hoxc*-6 (B), *Hoxa*-4 (C) and *Hoxa*-3 (D) as probes. h, heart; l, liver; my, myelencephalon; met, metencephalon; sc, spinal cord. pv 2,8,11 prevertebrae 2,8,11. Scale bar, 0.2 mm.

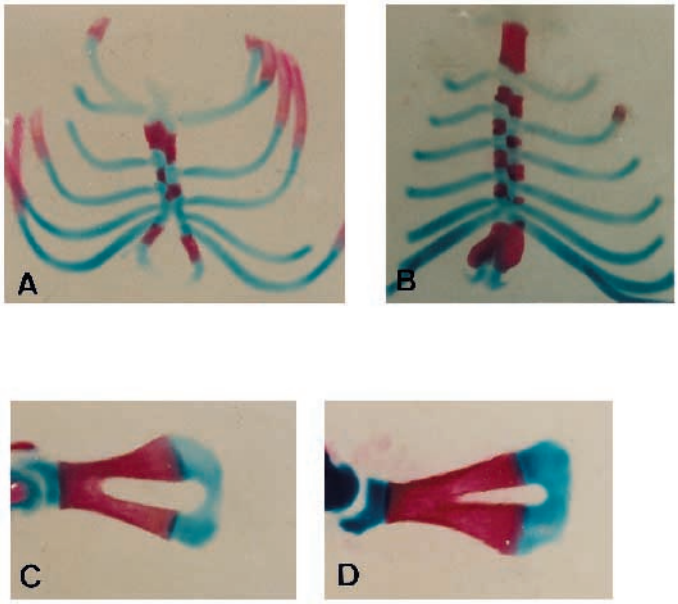

Fig. 5. Skeletal defects in 17.5 d.p.c. RA-treated *M33–/–* mice. (A,B) Ventral view showing the sternum region. (A) In the homozygotes, the first and the second thoracic ribs are fused to the sternum at the top of the manubrium sterni. The last two sternebrae are fused and the xiphoid process is split in two. (B) M33+/– sternum region; note the 'crankshaft sternum'; this phenotype has never been observed in non RA-treated mice. (C) Effect of RA on scapula malformation. RA-treated deficient mice as compared to non-treated *M33–/–* animals (D). Note the increased size of the hole in the RA-treated mutant mice.

levels in the embryonic liver and can transit between the immature DN (CD4–8– IL2R+), DP (CD4+8+) and mature SP(CD4+ or CD8+) stages, but that they generate far fewer mature T cells. Furthermore, they indicate that this failure to expand is an inherent property of the *M33–/–* thymocytes rather than a consequence of compromised health of the mice or generalized impairment of the thymic environment.

Analysis of cellular proliferation defects in *M33* mutant mice

In order to determine whether proliferation defects are present in other cell types in mutant mice, proliferation assays were performed on splenocytes and fibroblasts. Thymidine incorporation assays with LPS-activated splenocytes derived from three weeks old mutant mice indicate that these cells also fail to proliferate (Fig. 7A). Similarly, cellular counts over a two week period reveal that the *M33–/–* derived fibroblasts obtained from 12.5 d.p.c. embryos are severely impaired in their capacity to expand (Fig. 7B).

DISCUSSION

In this study, we have generated a mouse mutant line in which the *M33* gene, a homologue of *Drosophila Polycomb*, has been deleted. The *M33*-deficient mice present severely retarded growth, perturbations of cellular proliferation for several cell types and homeotic transformations of vertebrae. In *Drosophila*, the early pattern of expression of the homeotic genes established by the maternal and segmentation genes is later maintained by the trx-G and the Pc-G genes. These genes are involved in the maintenance respectively of the active or repressed state of expression of the homeotic genes in the appropriate segments. Loss of function in these groups of genes results in ectopic (Pc-G) or the loss (trx-G) of expression of the homeotic genes and, consequently, in homeotic transformations. In mice, as in *Drosophila, Hox* genes regulate organisation of the body plan (reviewed by McGinnis and Krumlauf, 1992). Similarly, it has been shown that mutant mice heterozygous for the trx-G gene homologue (*Mll*) present anterior and posterior transformation

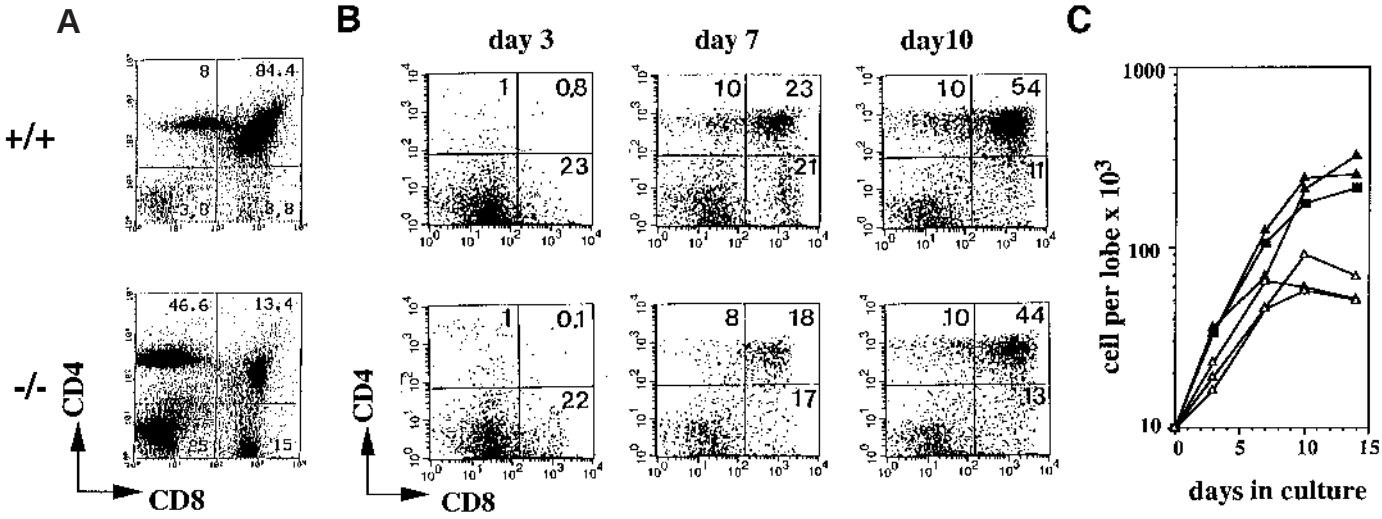

Fig. 6. (A) Representative flow cytometric analysis of thymocyte populations from 3-week-old *M33–/–* and wild-type mice stained to reveal CD4 and CD8 distribution. (B,C) Kinetics of T cell recolonisation in in vitro thymic organ cultures reconstituted with 12.5 d.p.c. liver from *M33–/–* (△-△), heterozygous *M33+/–* (■-■) and wild-type *M33+/+*(▲-▲) mice. The numerical values displayed in the quadrants of each cytogram show the mean proportion of each T cell subset expressed as a percentage of total viable cells. (C) The number of lymphocytes recovered per thymic lobe at each time point represents a mean of three independent determinations for cultures established from six mice. Unrecolonised, control thymuses contained $<10^4$ cells per lobe and, therefore, are omitted.

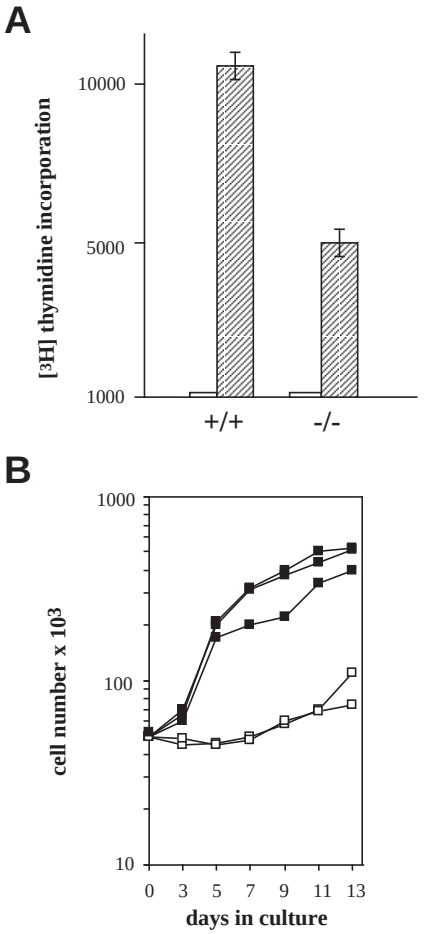

Fig. 7. Proliferation assays on splenocytes and fibroblasts from M33 mutant mice. (A) [^{3}H]thymidine incorporation was analysed on *M33+/+* and *M33–/–* splenocytes 48 hours after LPS activation; the proliferative response of the cells derived from the M33 mutant appears at least twofold less intense than the control cells. (B) Examination of growth of embryonic fibroblasts from wild-type (■–■) or *M33–/–* (□–□) 12.5 d.p.c. embryos. Cellular counts were completed over a two-week period.

of the axial skeleton and that null mutant mice fail to maintain the expression of the *Hox* genes at day 10 of development (Yu et al., 1995). Mutant mice for the Pc-G genes *mel-18* and *bmi-1* show axial posterior transformations and an anterior shift in the expression boundary of a subset of *Hox* genes (Akasaka et al., 1996; van der Lugt et al., 1994, 1996).

Homeotic transformations in *M33–/–* mice

The homeotic transformations observed in *M33–/–* mice (Table 1; Fig. 2) are reminiscent of homeotic transformations described for several mouse *Hox* gene mutants. Among loss-of-function mutants, for example, the *Hoxc-8* mutant mice present an anterior transformation as seen by the generation of an extra pair of ribs from the first lumbar vertebra (Le Mouellic et al., 1992); *Hoxb-4* mutant mice show partial posterior transformation of the atlas to the axis and sternal malformations (Ramirez-Solis et al., 1993). In *Hoxa-5* mutant mice, there is a posterior transformation of the cervical vertebra (C7) into the first thoracic vertebra (T1). Similarly homeotic transformations of the axial skeletal structures occur in gain-of-function mutants generated for *Hox* genes. The ectopic expression of *Hoxd-4* induces posterior skeletal transformations as seen by ectopic neural arches and the absence of the supra-occipital and exoccipital bones as well as a fusion of the atlas and the axis (Lufkin et al., 1992). Transgenic mice overexpressing the *Hoxa-7* gene show also posterior transformations of the axial skeleton as the atlas and the axis present characteristics of more posterior vertebra (Kessel et al., 1990).

The craniocervical transformations seen in the *M33*-deficient mice are, however, most similar to those reported in *Hoxd-3* null mutant mice (Condie and Capecchi, 1993). To explain the defects observed in *Hoxd-3–/–* mice, Condie and Capecchi suggested a model in which *Hoxd-3* regulates the proliferation rate of precursor cells. In agreement with this model, it has been shown that several *Hox* genes are involved in controlling cell proliferation (Care et al., 1994; Sauvageau et al., 1994; Sordino et al., 1995). Our results on the altered proliferation potential of different cell types as well as the cervical defects detected in the *M33–/–* mice are consistent with this model and support the notion that the relative dosage of the HOX proteins is critical for both proliferation and patterning processes (Condie and Capecchi, 1993). It has been shown that compound mutant mice for the *Hoxd-3/Hoxa-3* genes show a complete loss of the atlas vertebra revealing synergistic interactions between these two genes (Condie and Capecchi, 1994). Since the malformations observed in the cervical region of the *M33* mutant mice correspond more to those of the *Hoxd-3* mutant than to those of the compound *Hoxd-3/Hoxa-3* mutants suggest that the loss of the M33 protein mostly acts on the rate of expression of the *Hoxd-3* gene in the craniocervical region (Condie and Capecchi, 1994).

The findings that homeotic transformations are seen over the entire A-P axis indicates that *M33* may control the level of expression of several other *Hox* genes. The transformations observed in the anterior part of the skeleton are consistently seen in all the *M33–/–* mice whereas the transformations located in the posterior part are less penetrant (Table 1); this suggests that the M33 protein might primarily affect the *Hox* genes located in the 3′ end of the complex. Alternatively, since Pc-G genes in *Drosophila* are involved in the regulation of gap genes (Pelegri and Lehmann, 1994), it is possible that in *M33–/–* mutant mice the initiation phase of expression of some *Hox* genes is altered leading to posterior transformations. Although a direct regulation of the *Hox* genes by M33 has yet to be established, the alterations observed in the specification of structures along the A-P axis in *M33* mutant mice are in accordance with the *Pc* gene function in *Drosophila*.

bmi-1 and *mel-18* mutant mice present posterior transformations of the axial skeleton as well as an anterior shift in the expression boundaries of several *Hox* genes. Some of these posterior transformations are very similar to those observed in the *M33* mutant mice. Similarly, in the *M33*-deficient mice, the *Hoxa-3* gene expression domain is shifted anteriorly. However, we have not detected modifications in the anterior boundaries of several other *Hox* genes in the *M33* mutant mice. This might reflect the different mechanisms used to maintain the *Hox* gene expression and vertebral identity in mice. It has been shown that the two Pc-G genes, *bmi-1* and *mel-18*, regulate common *Hox* targets**.** It is possible that, in the absence of the M33 product, those genes still sustain some of the *Hox* gene domain of expression in their normal boundaries but that their level of

expression is not properly maintained. Since *bmi-1* and *mel-18* also regulate specific *Hox* genes, it is possible that *M33* controls the anterior limit of expression of *Hox* genes unaffected in *bmi-1* and *mel-18* mutant mice (Akasaka et al., 1996; van der Lugt et al., 1996). Alternatively, since we have used F_1 mice from a cross between 129/ola and BALB/C to obtain M33–/– mice, it is possible that the hybrid background might influence the Hox boundaries.

Pc-G gene products are thought to participate in the formation of large protein complexes, which promote the formation of condensed chromatin along specific chromosomal regions leading to a heritable repression of the HOM-C genes (Paro, 1990). In this model, the Pc-G proteins are thought to form a compacted chromatin structure that prevent interactions between DNA and DNA-binding proteins. This chromatin model implies that all transcription factors should be excluded from DNA in this repressed state. However, it has been recently shown in *Drosophila* (McCall and Bender, 1996) that, while the yeast GAL4-dependent transcription is inhibited by Pc, T7 RNA polymerase is not, implying that the compacted chromatin model for Pc-G repression is not completed by a simple exclusion of all the transcription factors. This repression could be achieved through a screening of the transcription factors by size or shape (McCall and Bender, 1996) or by nuclear compartmentalization whereby Pc-G repressed chromatin is maintained in an inactive region of the nucleus (Paro, 1993).

Effects of retinoic acid on *M33* mutant embryos

In mouse, the proper expression of several *Hox* genes is dependent on multiple RA response elements. For example, RAREs have been found in the *Hoxa-1* (Langston and Gudas, 1992) and *Hoxd-4* (Popperl and Featherstone, 1993) genes and mediate an up-regulation in response to ectopic doses of RA in cultured cells. Two enhancers 3′ of the mouse *Hoxb-1* have been identified, which are required for the proper expression of *Hoxb-1* (Marshall et al., 1994; Studer et al., 1994) and mediate the early ectopic response to RA. The enhancer that controls the RA response and regulates the expression of *Hoxb-1* in the neuroectoderm contains a RARE: point mutations in the RARE abolish the expression of the *Hoxb-1* gene in the neuroectoderm demonstrating that this RARE is essential for the correct expression of the *Hoxb-1* gene.

Our results with RA treatment on skeletal transformations in *M33* mutant mice suggest an interaction between RA activation pathway and *M33*. It is possible that the M33 protein might control the accessibility to the RAREs defined in the regulatory regions of some *Hox* genes during normal development. The absence of *M33* might allow those elements to be inappropriately accessible for transcription leading to misexpression or ectopic *Hox* genes expression. Whether RA-treated *M33–/–* embryos present extended shifts in the anterior limit of expression or overexpression of some *Hox* genes will require extensive analysis of several *Hox* genes that have been found to be directly responsive to RA via their RARE at different time points of development.

During gastrulation, vertebrate *Hox* genes are transcribed in a temporal sequence that is correlated to their position in the complex (temporal colinearity) (Dollé et al., 1989, Duboule and Morata, 1994; Gaunt and Strachan, 1996). It has been proposed that this 3′ to 5′ progressive opening of the Hox complexes might be achieved through a change in the chromatin configuration (Dollé et al., 1989). Our results support this proposal and suggest that this change might be mediated by Pc-G function. In this view, transition from an inactive chromatin state to an active state would allow critical *Hox* promoter regions (i.e. RAREs) to be accessible to specific activators or repressors. This suggests a fundamental difference between vertebrate and fly in activation of the *Hox* genes: in vertebrates, the *Hox* complexes are progressively opened to transcription while, in *Drosophila*, it is progressively closed during development (van der Hoeven, 1996).

Functional interactions between Pc-G genes

Mutant mice for the *bmi-1* and for *mel-18* genes show proliferation abnormalities and posterior transformations similar to the *M33–/–* mice indicating that this group of genes might interact in regulating the *Hox* complexes in mice. However, the specific axial transformations observed in *M33–/–* mice demonstrate that the *M33* gene has distinct, as well as common, *Hox* targets. It has been shown on polytene chromosomes in *Drosophila* that the Pc-G proteins are co-localized at many sites (DeCamillis et al., 1992). In *Xenopus* embryos, XPOLYCOMB and XBMI-1 proteins are able to interact with each other (Reijnen et al., 1995). Furthermore, stronger posterior transformations are observed in *Drosophila* mutant for two or more Pc-G genes (Jürgens, 1985). Consequently, one would expect extended posterior transformations and extended shifts in the *Hox* boundaries in double Pc-G mutant in mice. *bmi-1+/–* and *M33+/–* mice are currently being intercrossed in order to test this hypothesis.

Role of *M33* in lymphopoïesis

Our results on thymocyte differentiation demonstrate that the M33 protein is not required for T cell maturation since CD4+ and CD8+ single positive cells expressing normal level of T-cell receptor are detected in the thymus of mutant mice. However, we have found that the *M33* gene is necessary for T cell precursors proliferation. Recently, another Pc-G protein (Hobert, 1996), ENX-1, has been isolated in mouse by virtue of its association with the protein encoded by the proto oncogene *vav*. *vav* mutant mice (Tarakhovsky et al., 1996) also display involuted thymi and an impaired proliferative response to lymphoid activation emphasizing the possibility that Pc-group proteins have a pivotal role in lymphocyte proliferation. Since Pc-G proteins are thought to form large protein complexes, it is possible that the M33 protein could exert its effects on lymphoid proliferation through the VAV protein in the thymus. On the other hand, it has been demonstrated that misregulation of some *Hox* genes leads to lymphocytes proliferative alteration (Perkins et al., 1990, Sauvageau et al., 1994). Then, it is possible that the thymocytes defects induced in the *M33* mutant mice could be due to an altered expression of some *Hox* genes.

This work was supported by grants from CNRS, ARC, GEFLUC and British Council. N. C. is supported by ARC and Fondation de France Fellowships. We thank M. Merkenschlager for helping with FACS analysis, P. Golstein, P. Naquet and P. Dollé for critical reading of the manuscript, M. Malissen and A. Gillet for instruction in ES cell culture and blastocyt injection techniques.

REFERENCES

Alkema, M. J., van der Lugt, N. M. T., Bobeldijk, R. C., Berns, A. and van

Lohuizen, M. (1995). Transformation of axial skeleton due to overexpression of *bmi-1* in transgenic mice. *Nature* **374**, 724-727.

Akasaka, T., Kanno, M., Balling, R., Mieza, M. A., Taniguchi, M. and Koseki, H. (1996). A role for *mel-18*, a Polycomb group-related vertebrate gene, during the anteroposterior specification of the axial skeleton. *Development* **122**, 1513-1522.

Bienz, M. and Müller, J. (1995). Transcriptional silencing of homeotic genes in *Drosophila*. *BioEssays* **17**, 775-784.

Brunk, B. P., Martin, E. C. and Adler, P. N. (1991). *Drosophila* genes *posterior sex combs* and *suppressor two of zeste* encode proteins with homology to the murine *bmi-1* oncogene. *Nature* **353**, 351-353.

Care, A., Testa, U., Bassani, A., Tritarelli, E., Montesoro, E., Samoggia, P., Cianetti, L. and Peschle, C. (1994). Coordinate expression and proliferative role of HOXB genes in activated adult T lymphocytes. *Mol. Cell. Biol.* **14**, 4872-4877.

Cohen, J. J. and Duke, R. C. (1984). Glucocorticoid activation of a calcium-dependent endonuclease in thymocyte nuclei leads to cell death. *J. Immunol.* **132**, 38-42.

Condie, B. G. and Capecchi, M. R. (1993). Mice homozygous for a targeted disruption of *Hox*d-3 (*Hox*-4.1) exhibit anterior transformations of the first and second cervical vertebrae, the atlas and the axis. *Development* **119**, 579-595.

Condie, B. G. and Capecchi, M. R. (1994). Mice with targeted disruptions in the paralogous genes hoxa-3 and hoxd-3 reveal synergistic interactions. *Nature* **370**, 304-306.

Conlon, R. A. and Rossant, J. (1994). Exogenous retinoic acid rapidly induces anterior ectopic expression of murine *Hox*-2 genes in vivo. *Development* **116,** 357-368.

DeCamillis, M., Cheng, N., Pierre, D. and Brock, H. W. (1992). The *polyhomeotic* gene of *Drosophila* encodes a chromatin protein that shares polytene chromosome-binding sites with *Polycomb*. *Genes Dev* **6**, 223-232.

Dollé, P, Izpisua-Belmonte, J. C., Falkenstein, H., Renucci, A. and Duboule, D. (1989). Coordinate expression of the murine Hox-5 complex homoeobox-containing genes during limb pattern formation. *Nature* **342**, 767-772.

Duboule, D. and Morata, G. (1994). Colinearity and functional hierarchy among genes of the homeotic complexes. *TIG* **10**, 358-364.

Duncan, I. and Lewis, E. B. (1982). Genetic control of body segment differentiation in *Drosophila*. In *Developmental Order: its Origin and Regulation* (ed. S Subtelny). pp. 553-554. New York: Liss

Gaunt, S. J. and Strachan, L. (1996). Temporal colineaity in expression of anterior Hox genes in developing chick embryos. *Developmental Dynamics* in press.

Gaunt, S. J., Sharpe, P. T. and Duboule, D. (1988). Spatially restricted domains of homeo-gene transcripts in mouse embryos: relation to a segmented body plan. *Development* **104 Supplement**, 169-179.

Hobert, O., Sures, I., Ciossek, T., Fuchs, M. and Ullrich, A. (1996). Isolation and developmental expression analysis of ENX-1, a novel mouse Polycomb group gene. *Mech. Dev.* **55**, 171-184.

Ingham, P. W. (1988). The molecular genetics of embryonic pattern formation in *Drosophila*. *Nature* **335**, 25-33.

Jürgens, G. (1985). A group of genes controlling the spatial expression of the *bithorax* complex in *Drosophila*. *Nature* **316**, 153-155.

Kennisson, J. A. (1993). Transcriptional activation of *Drosophila* homeotic genes from distant regulatory elements. *Trend Genets* **9**, 75-79.

Kessel, M. and Gruss, P. (1991). Homeotic transformation of murine vertebrae and concomitant alteration of *Hox* codes induced by retinoic acid. *Cell* **67**, 89-104.

Kessel, M., Balling, R. and Gruss, P. (1990). Variations of cervical vertebrae after expression of a Hox-1.1 transgene in mice. *Cell* **61**, 301-308.

Krumlauf, R. (1994). *Hox* genes in vertebrate development. *Cell* **78**, 191-201.

Langston, A. W. and Gudas, L. J. (1992). Identification of a retinoic acid responsive enhancer 3′ of the murine homeobox gene Hox-1.6. *Mech. Dev.* **38**, 217-227.

Le Mouellic, H., Lallemand, Y. and Brulet, P. (1992). Homeosis in the mouse induced by a null mutation in the *Hox*-3.1 gene. *Cell* **69**, 251-264

Lufkin, T., Mark, M., Hart, C. P., Dollé, P., LeMeur, M. and Chambon, P. (1992). Homeotic transformation of the occipital bones of the skull by ectopic expression of a homeobox gene. *Nature* **359**, 835-841.

Marshall, H., Studer, M., Pöpperl, H., Aparicio, S., Kuroiwa, A., Brenner, S. and Krumlauf, R. (1994). A conserved retinoic acid response element required for early expression of the homeobox gene *Hoxb-1*. *Nature* **370**, 567-571.

McCall, K. and Bender, W. (1996). Probes of chromatin accessibility in the *Drosophila* bithorax complex respond differently to Polycomb-mediated repression. *EMBO J* **15**, 569-580.

McGinnis, W. and Krumlauf, R. (1992). Homeobox genes and axial patterning. *Cell* **68**, 283-302.

Messmer, S., Franke, A. and Paro, R. (1992). Analysis of the functional role of the *Polycomb* chromo domain in *Drosophila melanogaster*. *Genes Dev.* **6**, 1241-1254.

Müller, J., Gaunt, S. and Lawrence, P. (1995). Function of the Polycomb protein is conserved in mice and flies. *Development* **121,** 2847-2852.

Paro, R. (1990). Imprinting a determined state into the chromatin of Drosophila. *Trends Genet.* **6**, 416-421.

Paro, R. (1993). Mechanisms of heritable gene repression during development of *Drosophila. Curr. Biol.* **5**, 999-1005.

Paro, R. and Hogness, D. (1991). The Polycomb protein shares a homologous domain with a heterochromatin-associated protein of *Drosophila. Proc. Natl. Acad. Sci. USA* **88**, 263-267.

Pearce, J. H., Singh, P. B. and Gaunt, S. J. (1992). The mouse has a *Polycomb*-like chromobox gene. *Development* **114**, 921-929.

Pelegri, F. and Lehmann, R. (1994). A role of *Polycomb* group genes in the regulation of gap gene expression in *Drosophila. Genetics* **136**, 1341-1353.

Perkins, A., Kongsuwan, K., Visvader, J., Adams, J. M. and Cory, S. (1990). Homeobox gene expression plus autocrine growth factor production elicits myeloid leukemia. *Proc. Natl. Acad. Sci. USA* **87**, 8398-8402.

Pirrotta, V. (1995). Chromatin complexes regulating gene expression in *Drosophila. Curr. Bio.* **5**, 466-472.

Popperl, H. and Featherstone, M. S. (1993). Identification of a retinoic acid response element upstream of the murine Hox-4.2 gene. *Mol. Cell. Biol.* **13**, 257-265.

Ramirez-Solis, R., Zheng, H., Whiting, J., Krumlauf, R. and Bradley, A. (1993). *Hoxb-4 (Hox2.6)* mutant mice show homeotic transformation of a cervical vertebra and defects in the closure of the sternal rudiments. *Cell* **73**, 279-294.

Reijnen, M. J., Hamer, K. M., den Blaauwen, J. L., Lambrechts, C., Schoneveld, I., van Driel, R. and Otte, A. P. (1995). *Polycomb* and *bmi-1* homologs are expressed in overlapping patterns in *Xenopus* embryos and are able to interact with each other. *Mech. Dev*. **53**, 35-46.

Sauvageau, G., Lansdorp, P. M., Eaves, C. J., Hogge, D. E., Dragowska, W. H., Reid, D. S., Largman, C., Lawrence, J. H. and Humphries, K. R. (1994). Differential expression of homeobox genes in functionally distinct CD34+ subpopulations of human bone marrow cells. *Proc. Natl. Acad. Sci. USA* **91**, 12223-12227.

Sordino, P., van der Hoeven, F. and Duboule, D. (1995). Hox gene expression in teleost fins and the origin of vertebrate digits. *Nature* **375**, 678-681.

Studer, M., Pöpperl, H., Marshall, H., Kuroiwa, A. and Krumlauf, R. (1994). Role of a conserved retinoic acid response element in rhombomere restriction of *Hoxb-1*. *Science* **265**, 1728-1731.

Tagawa, M., Sakamoto, T. Shigemoto, K., Matsubara, H., Tamura, Y., Ito, T., Nakamura, I., Okitsu, A., Imai, K. and Taniguchi, M. (1990). Expression of novel DNA-binding protein with zinc finger structure in various tumor cells. *J. Biol. Chem*. **265**, 20021-20026.

Tarakhovsky, A., Turner, M., Schaal, S., Mee, P. J., Duddy, L. P., Rajewsky, K. and Tybulewicz, V. L. (1995). Defective antigen receptor-mediated proliferation of B and T cells in the absence of Vav. *Nature* **374**, 467-470.

van der Hoeven, F., Zakany, J. and Duboule, D. (1996). Gene transpositions in the HoxD complex reveal a hierarchy of regulatory controls.*Cell* **85**, 1025-1035.

van der Lugt, N. M. T. et al. (1994). Posterior transformation, neurological abnormalities, and severe hematopoietic defects in mice with a targeted deletion of the *bmi-1* proto-oncogene. *Genes Dev.* **8**, 757-769.

van der Lugt, N. M. T., Alkema, M., Berns, A. and Deschamps, J. (1996). The *Polycomb*-group homolog Bmi-1 is a regulator of murine *Hox* gene expression. *Mech. Dev.* **58**, 153-164.

van Lohuizen, M., Frasch, M., Wientjens, E. and Berns, A. (1991). Sequence similarity between the mammalian *bmi-1* proto-oncogene and the *Drosophila* regulatory genes *Psc* and *Su(z)2*. *Nature* **353**, 353-355.

Wedeen, C., Harding, K. and Levine, M. (1986). Spatial regulation of *Antennapedia* and *Bithorax* gene expression by the *Polycomb* locus of *Drosophila*.*Cell* **44**, 739-748.

Yu, B. D., Hess, J. L., Horning, S. E., Brown G. A. and Korsmeyer, S. J. (1995). Altered *Hox* expression and segmental identity in Mll-mutant mice. *Nature* **378**, 505-508.

Zink, B., Engström, Y., Gehring, W. J. and Paro, R.(1991). Direct interaction of the *Polycomb* protein with *Antennapedia* regulatory sequences in polytene chromosomes of *Drosophila melanogaster*. *EMBO J*. **10**, 153-162.

(Accepted 7 November 1996)